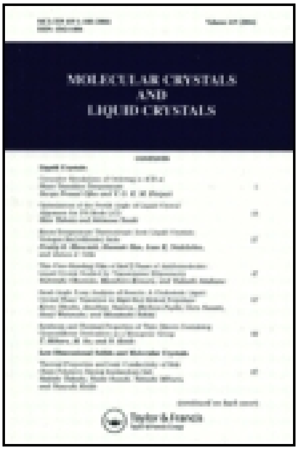

Molecular Crystals and Liquid Crystals
Publication details, including instructions for authors and subscription information:
http://www.tandfonline.com/loi/gmcl20

Liquid Crystal Lens of Two Liquid Crystal Layers

Mao Ye* [a] & Susumu Sato [a]

[a] Department of Electrical and Electronic Engineering, Akita University, Japan

Version of record first published: 18 Oct 2010

Mol. Cryst. Liq. Cryst., Vol. 422, pp. 197/[467]–207/[477], 2004

ISSN: 1542-1406 print/1563-5287 online
DOI: 10.1080/15421400490502535

LIQUID CRYSTAL LENS OF TWO LIQUID CRYSTAL LAYERS

Mao Ye and Susumu Sato*
Department of Electrical and Electronic Engineering
Akita University, 1-1 Tegatagakuen-cho
Akita 010-8502, Japan

Liquid crystal lenses (LCL) of two liquid crystal (LC) layers with parallel and orthogonal optic axes are built. The LCL of two LC layers with parallel optic axes is designed to obtain larger focusing power, and that with orthogonal optic axes is to focus light wave of arbitrary polarizations. The focal lengths of both LCLs can be controlled by external voltages.

Keywords: liquid crystal lens; tunable focal length; two liquid crystal layers

INTRODUCTION

The focal length of a liquid crystal lens (LCL) is tunable by external electric fields, and it is hopeful for LCLs to replace traditional lenses in some applications. Several kinds of LCL have been proposed [1–7]. Recently we have reported an LCL with one hole-patterned electrode [6]. The hole-patterned electrode is placed on the outer side of the liquid crystal (LC) cell, that is, between the hole-patterned electrode and the LC layer there is an insulator layer. With this structure, the nonuniform electric field can distribute in a large area in the LC layer, and LCL of large size can therefore be fabricated. The outside placing of the hole-patterned electrode also makes it easy to build an LCL with two LC layers. The two LC layers share the common hole-patterned electrode. A two-LC-layer LCL has either a much larger focusing power or ability of focusing light wave of arbitrary polarizations. In this paper we report two kinds of two-LC-layer LCLs. In one of the LCLs the optic axes of the two LC layers are in the same direction, and

This work was supported in part by Akita Prefecture Collaboration of Regional Entities for the Advancement of Technological Excellence, JST.

*Corresponding author. Tel.: +81-18-889-2483, Fax: +81-18-837-0406, E-mail: maoye@ipc.akita-u.ac.jp

the focusing power increases. In the other LCL, the optic axes are perpendicular. The LCL can focus incident light beam of arbitrary polarizations.

LCL CELL STRUCTURES

The side view of the structure of the LCL cell is shown in Figure 1. The two transparent electrodes are electrically connected and the hole-patterned Al electrode in the middle of the cell is shared by the two LC layers. Nonuniform electric fields nearly centrosymmetrical in the two LC layers are produced by the voltage V across the transparent electrodes and the common Al electrode. The LC material used in this work is Merck E44. The thickness of the LC layers and that of the glass substrates between the hole-patterned electrode and the LC layers are 130 μm and 1.3 mm, respectively. The hole pattern diameter is 7.0 mm. A diaphragm with a diameter of 5.0 mm is fixed on the cell so that only the central part of an incident light beam passes through the cell. The frequency of the applied AC voltage is 1 kHz.

The Al electrode and the four surfaces contacting the LC films viewed from the top are illustrated in Figure 2. The surfaces are coated with Polyimide (PI) and rubbed. The arrows in the figures represent the rubbing directions. In the LCL of rubbing mode shown in Figure 2(a), the initial alignments of the directors in the bottom and top LC layers are parallel and the optic axes of the two LC layers are parallel. In the LCL of rubbing mode shown in Figure 2(b), the initial alignments of the directors in the bottom and top LC layers are perpendicular, and the two LC layers are of orthogonal optic axes. The two-LC-layer LCL with rubbing mode of Figure 2(a) is designed to obtain a larger focusing power, and that with rubbing mode of Figure 2(b) are to focus incident light beam of arbitrary polarizations.

LCL OF TWO LC LAYERS WITH PARALLEL OPTIC AXES

Due to the introduction of additional electrodes and polarized dielectrics, in a two-LC-layer LCL, the reorientation of the LC directors is surely differ-

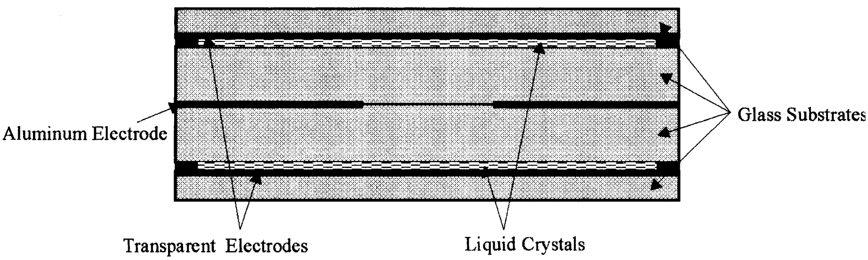

FIGURE 1 Cell structure.

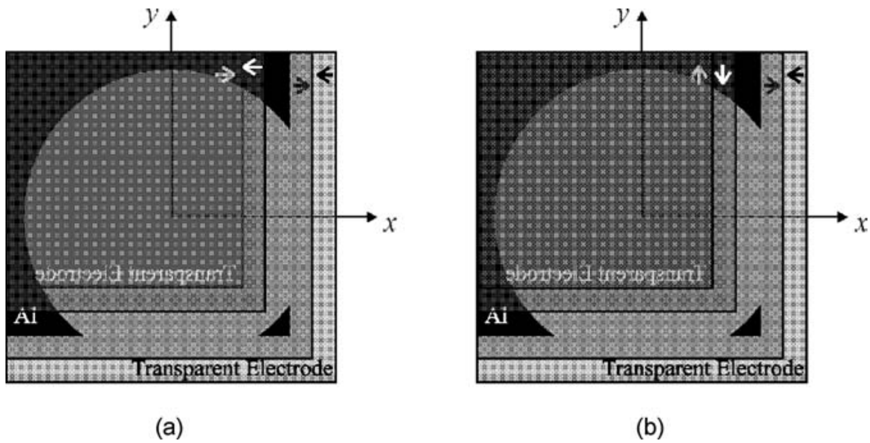

FIGURE 2 Rubbing modes.

ent from that in a one-LC-layer LCL. To investigate the properties of the two-LC-layer LCL in detail, we first make two one-LC-layer LCLs, and measure the properties of each LCL. Then we overlap the two cells to form a two-LC-layers LCL as shown in Figure 1, and also measure its properties.

At various applied voltages, the phase profile of a He-Ne laser beam after traversing the LC cells is measured using the following interference method. The LC cells are placed between two crossed polarizers with its rubbing direction at 45° to each polarizer. An incident light wave is first divided by the front polarizer into an ordinary wave (o-wave) and an extraordinary one (e-wave). The rear polarizer recombines the two waves and the two wave interfere. For the LC thickness is uniform and the ordinary wave experiences a spatially constant phase shift, from the interference pattern the spatial variance of the phase shift experienced by the e-wave can be deduced. The phase difference between two neighboring interference fringes is 2π.

Figure 3 shows the interference patterns for the two one-LC-layer cells when a voltage of $90\,V_{rms}$ is applied, and Figure 4 shows that for the two-LC-layers cell. From the patterns the phase profiles are obtained and shown in Figure 5. The dots are the measurements and the solid lines are quadratic fittings. It can be seen that the phase profiles are nearly quadratically distributed. So the LCLs behave well in mapping the incident plane waves into spherical ones. The two-LC-layer LCL has a larger phase difference between the edge and the center than the one-LC-layer LCLs, indicting the former has a larger power. Experiment shows that for a one-LC-layer LCL the phase profile of the light wave maintains a

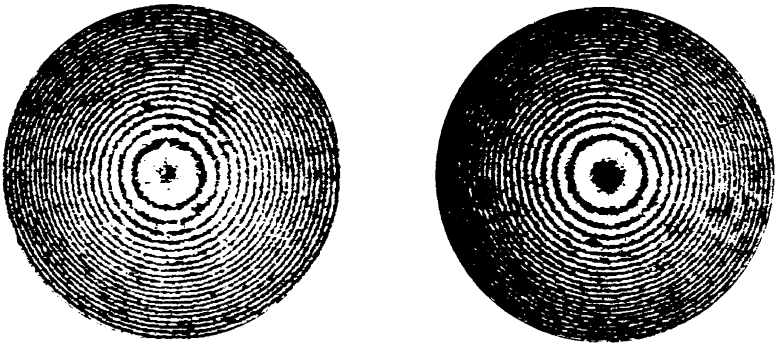

FIGURE 3 Interference patterns of two one-LC-layer LCLs.

nearly quadratic form in a voltage range of $V = 40 - 130\,\mathrm{V_{rms}}$, and for a two-LC-layer LCL the voltage range is $V = 50 - 125\,\mathrm{V_{rms}}$. For a lens, the phase transformation of quadratic form can be expressed as

FIGURE 4 Interference pattern of LCL of two LC layers with parallel optic axes.

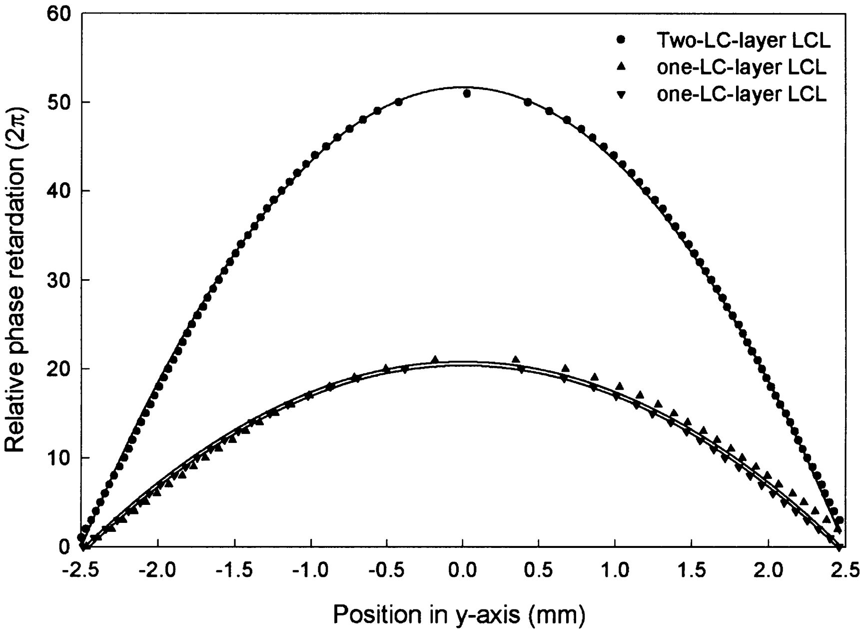

FIGURE 5 Phase profiles of LCL of two LC layers with parallel optic axes and one-LC-layer LCLs.

$\exp[-jk(x^2+y^2)/\,(2f)]$, where k is the wave number of the light wave, and f the focal length. From the measured phase distributions, the powers $P = 1/f$ of the LCLs at various V are deduced.

Figure 6 shows the powers as functions of the applied voltage. It is not surprised to see that the two one-LC-layer LCLs have nearly the same powers at the same voltage, because the two LCLs are made almost identically, and that the two-LC-layer LCL is more powerful than the one-LC-layer LCLs. It is notable that the power of the two-LC-layer LCL is larger than two times of that of a one-LC-layer LCL. The reason will be discussed later.

The high optical quality, large size, and strong power of the LCLs in this study make them already be able to be used as devices of image formation. The image formation by the two-LC-layer LCL is demonstrated. A printed paper is placed at one side of the LCL at a distance shorter than the minimum focal length, and a camera is located at the other side to capture the image of the words on the paper formed by the LCL. A polarizing plate is placed before the camera lens so that only the component of the light wave polarized parallel to x-axis can enter the camera. At various voltages, the photos taken are shown in Figure 7. The power of the LCL is controlled

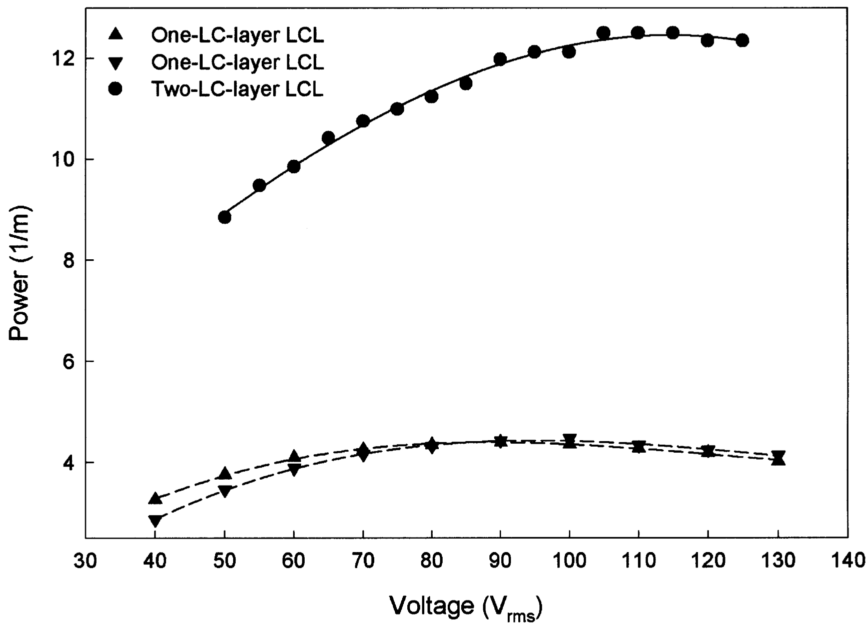

FIGURE 6 Powers of LCL of two LC layers with parallel optic axes and one-LC-layer LCLs at various voltages.

by the voltage. In the absence of an external voltage, the camera directly captures the words on the paper. At $V = 60$ and $90\,V_{rms}$, the camera captures enlarged virtual images of the words. At $90\,V_{rms}$ the image is larger than that at $60\,V_{rms}$, because the focal length is shorter at $90\,V_{rms}$.

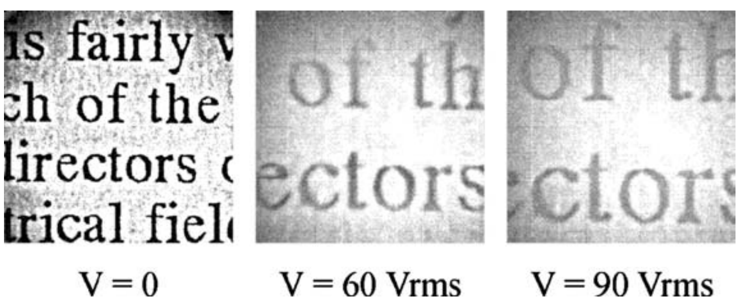

FIGURE 7 Images formed by LCL of two LC layers with parallel optic axes at various voltages.

LCL OF TWO LC LAYERS WITH ORTHOGONAL OPTIC AXES

For the two LC layers have optic axes perpendicular to each other, the LCL can focus a light beam of arbitrary polarizations. The top and bottom LC layers focus the two components of the incident light wave separately. The x-component of the light wave is an o-wave in the top layer and an e-wave in the bottom layer, and is focused by the bottom LC layer; the y-component, on the other hand, is an e-wave in the top layer and an o-wave in the bottom layer, and is focused by the top LC layer. Figure 8 shows the intensity distribution of a focused He-Ne laser beam linearly polarized in the 45° direction near the focal plane at $V = 110$ V_{rms}. The full-width at half maximum (FWHW) of the focus is approximately 150 μm.

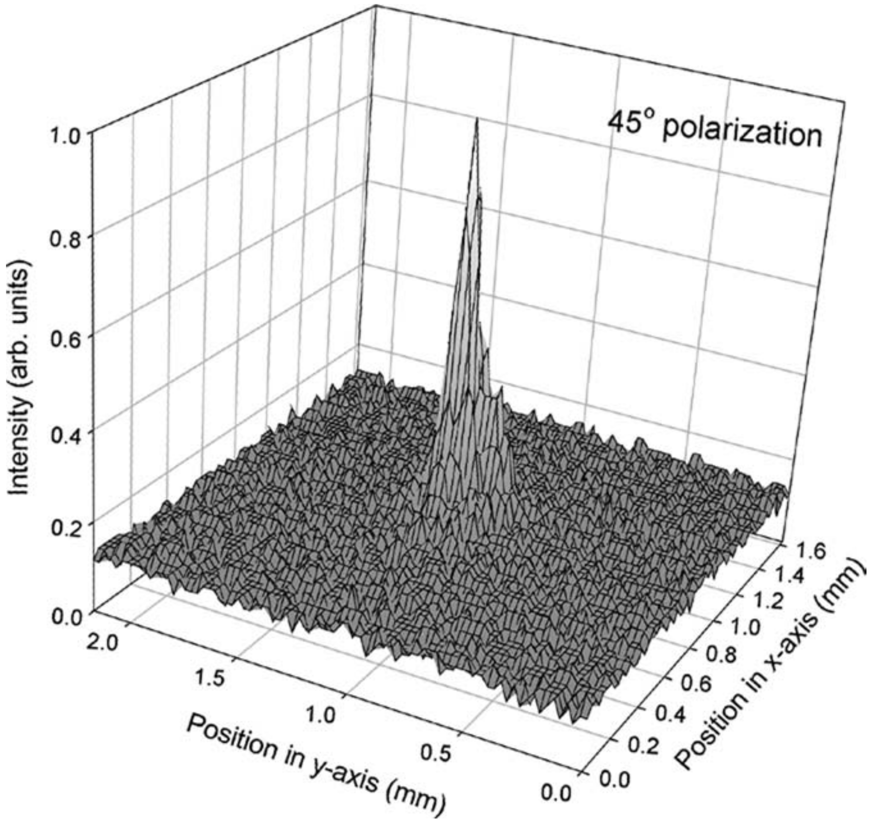

FIGURE 8 Intensity distribution in focal plane of light beam 45° polarized focused by LCL of two LC layers with orthogonal optic axes.

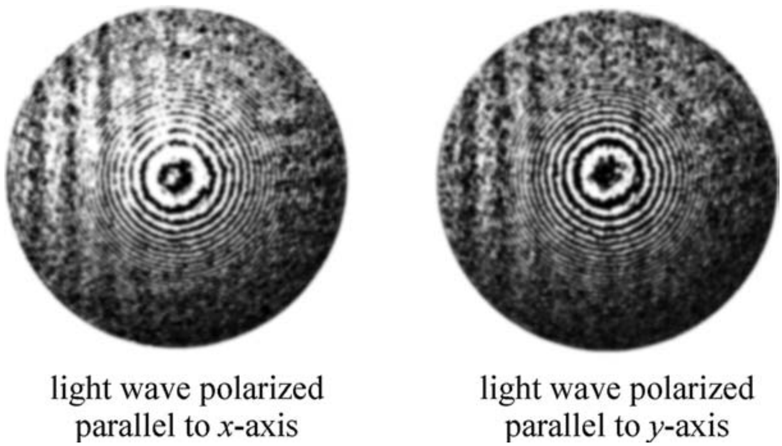

FIGURE 9 Interference patterns of LCL of two LC layers with orthogonal optic axes.

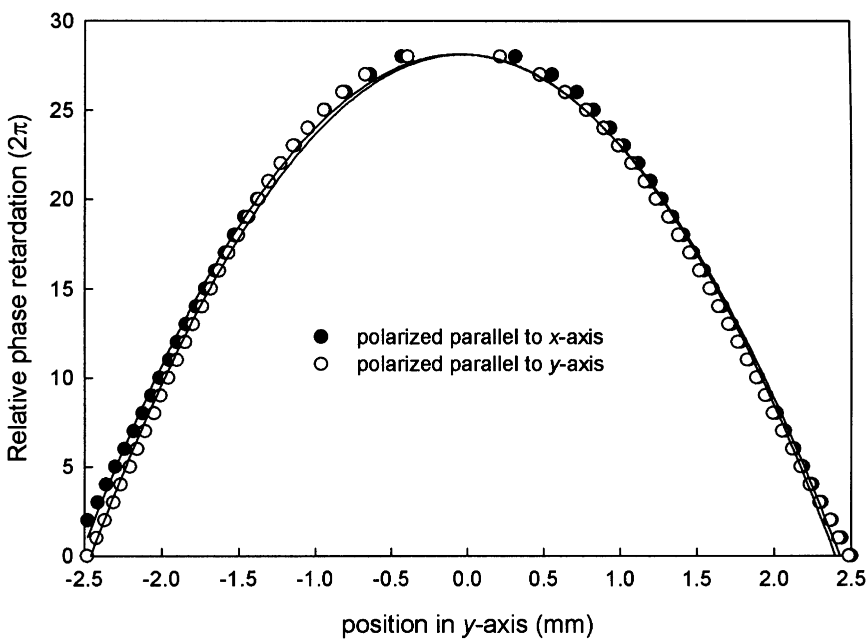

FIGURE 10 Phase profiles of LCL of two LC layers with orthogonal optic axes.

Due to the orthogonal optic axes, the interference method used in the study of the LCL of two LC Layers with parallel optic axes is no longer valid for measuring the phase profile of the incident light beam. The phase is observed by a Mach-Zehnder interferometer. The interference patterns for light beams polarized parallel to the x- and y-axis at $110\,V_{rms}$ are shown in Figure 9. The phase distributions deduced from the interference patterns are shown in Figure 10. The dots are the measurements and the solid lines the quadratic fitting. Again, it can be seen the phases are quadratically distributed. Experiment shows that in a range of $V = 90 - 140\,V_{rms}$, the phase profiles of nearly quadratic forms maintain. The deduced powers of the LCL as functions of voltage are shown in Figure 11. As would be expected, the powers for light waves parallel to x- and y-axis are very close.

Figure 12 shows images formed by the LCL at various voltages. The image size changes with the voltage. For the LCL can deal with light wave of arbitrary polarizations, no polarizing plate is used in the experiment.

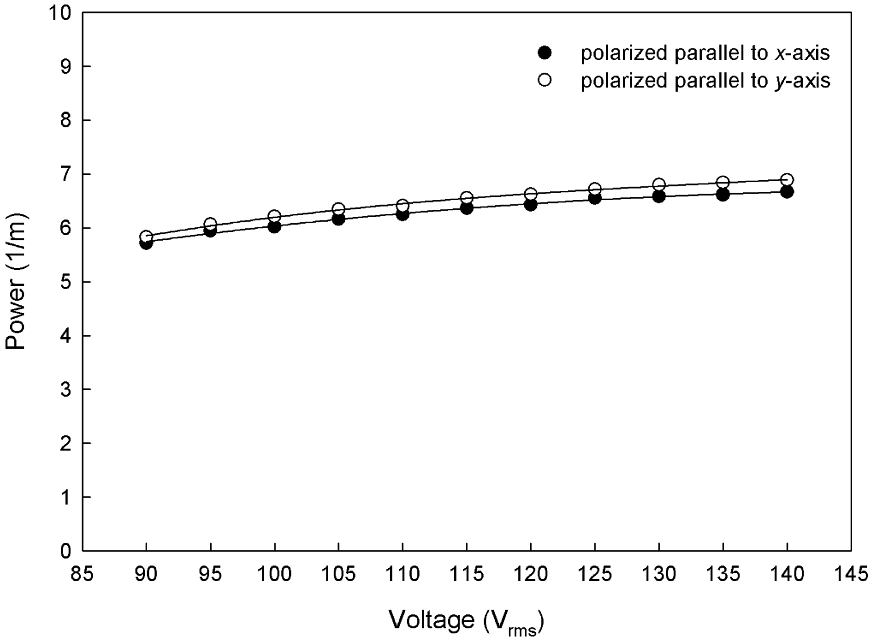

FIGURE 11 Powers of LCL of two LC layers with orthogonal optic axes at various voltages.

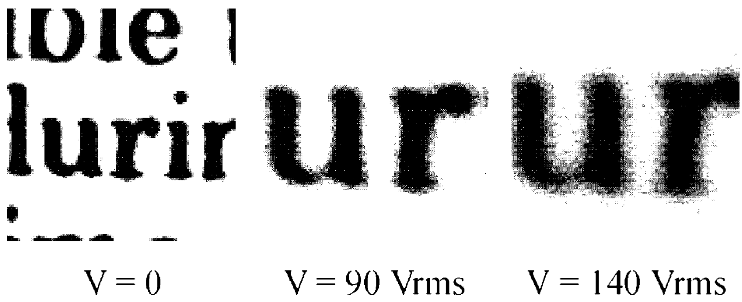

FIGURE 12 Images formed by LCL of two LC layers with orthogonal optic axes.

DISCUSSION

The focusing power of a tight combination of two thin glass lenses is the sum of those of the individual lens [8]. In the case of an LCL of two LC layers with parallel optic axes, the power is larger than the sum. It is found that the power of one LC layer is increased after the LC layer is combined with another LC layer to form a two-LC-layer LCL. The powers of the LCLs used in the experiment at various voltages are listed in Table 1. It can be seen that the power of the LCL of two LC layers with orthogonal axes is very close to half of that of the LCL of two LC layers with parallel axes. This is understandable because they in fact represent the average power of one LC layer in a two-LC-layer LCL. The power of the LCL of two LC layers with orthogonal axes and half of the power of the LCL of two LC layers with parallel axes are, however, larger than that of the one-LC-layer LCL. The average power increase of one LC layer in a two-LC-layer LCL of approximately 34%, 40%, 48%, and 53% at voltage of 90, 100, 110, and 120 V_{rms}, respectively, is seen.

TABLE 1 Comparison of Powers of Two-LC-Layer and One-LC-Layer LCLs at Various Voltages

V (V_{rms})			90	100	110	120
P (1/m)	Two-LC-layer LCL (parallel optic axes)	Total	12.0	12.1	12.5	12.4
		One LC layer (Total/2)	6.0	6.1	6.3	6.2
	Two-LC-layer LCL (orthogonal optic axes)		5.8	6.2	6.4	6.6
	One-LC-layer LCL (average)	4.4	4.4	4.3	4.2	

The power increase of one LC layer in a two-LC-layer LCL can be attributed to the electric accumulated charges at the other side of the hole-patterned electrode. In particular, the free electric charges in the electrode at the other side weaken the electric field in the central part of the LC layer. The directors near the center do not rotate so much as in the case that the LC layer is alone. So the gradient distribution of the effective refractive index becomes steeper, and the focusing power of the LC layer increases when the other LC layer is combined in the cell.

CONCLUSION

Two kinds of two-LC-layer LCLs are built. The LCL of two LC layers with parallel optic axes has power about 3 times larger than a one-LC-layer LCL. The LCL of two LC layers with orthogonal optic axes can focus light wave of arbitrary polarizations, and its power also increases. Both LCLs have focal lengths electrically tunable, and are of high optical quality. Their uses as image formation devices are successfully demonstrated.

REFERENCES

[1] Sato, S. (1979). *Jpn. J. Appl. Phys.*, *18*, 1679.
[2] Nose, T. & Sato, S. (1989). *Liq. Cryst.*, *5*, 1425.
[3] Naumov, A. F., Loktev, M. Yu., Guralnik, I. R., & Vdovin, G. (1998). *Opt. Lett.*, *23*, 992.
[4] Scharf, T., Kipfer, P., Bouvier, M., & Grupp, J. (2000). *Jpn. J. Appl. Phys.*, *39*, 6629.
[5] Commander, L. G., Day, S. E., & Selviah, D. R. (2000). *Opt. Commun.*, *177*, 157.
[6] Ye, M. & Sato, S. (2002). *Jpn. J. Appl. Phys.*, *41*, L571.
[7] Wang, B., Ye, M., Honma, M., Nose, T., & Sato, S. (2002). *Jpn. J. Appl. Phys.*, *41*, L1232.
[8] Born, M. & Wolf, E. (1999). *Principles of optics*, Press of University of Cambridge: Cambridge, UK.